

Synthesis and characterization of aluminum/iron – pillared bentonite catalysts for empty fruit bunches biomass gasification

Ria Komala^{1,2} , Dedi Rohendi³, Fakhili Gulo¹, Muhammad Faizal^{4*}

¹ Environmental Science Doctoral Study Program, Graduate School, Universitas Sriwijaya, Jl. Padang Selasa, No. 524, Bukit Besar, Palembang 30139, Sumatera Selatan, Indonesia.

² Chemical Engineering Department, Faculty of Engineering, Universitas Tamansiswa, Jl. Tamansiswa No. 261 20 Ilir D. I, Ilir Tim. I, Kota Palembang, Sumatera Selatan, Indonesia

³ Chemistry Department, Faculty of Mathematics and Natural Sciences, Universitas Sriwijaya, Jl. Raya Palembang-Prabumulih Km 32 Indralaya, Ogan Ilir, Sumatera Selatan 30662, Indonesia

⁴ Chemical Engineering Department, Faculty of Engineering, Universitas Sriwijaya, Jl. Raya Palembang Prabumulih Km 32 Indralaya, Ogan Ilir, Sumatera Selatan 30662, Indonesia

* Corresponding author's e-mail: muhammadfaizal@unsri.ac.id

ABSTRACT

Biomass gasification, such as the gasification of empty fruit bunches (EFB), is a promising method for renewable energy production. However, its efficiency remains limited due to high tar formation, incomplete carbon conversion, and the lack of effective catalysts. This study aims to synthesize a catalyst from bentonite pillared with aluminum (Al) and iron (Fe) to address these challenges and enhance gasification efficiency. The catalyst was characterized using FTIR, SEM, EDS, and XRD, and gasification was performed at 550 °C with catalyst concentrations of 1.25% and 2.5%. FTIR confirmed the formation of Al-O and Fe-O bonds, while SEM revealed a smooth, porous surface with evenly distributed metals. The material exhibited a porosity of 54.36% and a pore volume of $7.448 \times 10^{-2} \text{ m}^3$. EDS recorded Al and Fe contents of 12.9% and 8.0%, respectively, and XRD confirmed the successful incorporation of metal pillars. XRD analysis showed significant structural changes, with metal-pillared bentonite achieving the highest crystallinity of 68.96% and an average crystal size of 22.152 nm, reflecting improved stability and catalytic performance. These modifications enhanced porosity and thermal stability, crucial for high-temperature applications. Gasification with the 2.5% catalyst increased H₂ content to 36.1%, CO to 19.7%, and reduced CO₂ to 1.2%. Carbon conversion efficiency reached 82.5%, and cold gas energy efficiency improved to 41.2%. In conclusion, Al/Fe-pillared bentonite enhanced gasification performance and produced high-quality syngas suitable for renewable energy applications.

Keywords: catalyst, bentonite, Al/Fe-pillared bentonite, characterization, biomass gasification.

INTRODUCTION

EFB are one of the abundant biomass wastes in Indonesia, the world's largest producer of palm oil (Windiastuti et al., 2022). However, this waste is often underutilized. In fact, EFB has significant potential to be processed into renewable energy through gasification (Makwana et al., 2023). Gasification is a thermochemical process that converts organic materials into synthesis gas (syngas), which can be utilized as fuel (Havilah et al., 2022). Despite its promising potential, the

implementation of this technology still faces several major challenges, such as low gasification efficiency, excessive tar formation, and incomplete carbon conversion. These challenges negatively impact both the quality and quantity of the produced syngas. To address these issues, breakthroughs are required to enhance the efficiency of the gasification process. One promising approach is the application of catalysts to optimize the performance of the gasification system.

Bentonite, an aluminosilicate material, has long been known for its adsorption capability and

high thermal stability, making it a promising candidate as a catalyst in biomass gasification (Borah et al., 2022). Modified bentonite, whether through acid activation or metal pillaring, has been shown to improve its adsorption capacity and catalytic activity. Acid activation increases the surface area and number of active sites on bentonite, while metal pillaring, such as using Al and Fe metals, can enhance catalyst stability, reduce tar formation, and improve gasification yields. Metal-pillared bentonite (Al/Fe) can enhance gasification efficiency by improving the physicochemical characteristics of the material, thus making it more effective in converting biomass waste into high-quality syngas.

Al and Fe metals were chosen as pillars in this study because both metals have advantages that can improve the catalytic performance of bentonite in biomass gasification. Aluminum (Al) is known for its light weight, good thermal stability, and its ability to form active compounds that can support gasification reactions. Iron (Fe), on the other hand, has strong catalytic properties and can enhance gasification efficiency by participating in gas shift reactions and syngas formation. The combination of these two metals is believed to improve catalyst stability, reduce tar formation, and increase gasification yields, making it an ideal choice for biomass gasification applications, especially for empty fruit bunch (EFB) and palm kernel shell (PKS) waste.

Previous studies have shown the potential of using bentonite as a catalyst in biomass gasification. For example, activating bentonite with sulfuric acid can increase its specific surface area and number of active sites, thus improving its adsorption capacity for pollutants and enhancing carbon conversion in gasification. Metal pillaring of bentonite with Al and Fe has also been shown to improve the thermal stability and catalytic capacity of bentonite. However, studies on the effects of metal pillaring in biomass waste gasification, especially EFB and PKS, are still limited (Aprianti et al., 2024). Some studies, such as those by Faizan and Song (2023), indicate that transition metal-based catalysts like Ni, Zn, and Co in biomass gasification can also improve gasification efficiency and syngas quality, such as the content of H₂ and CO (Faizan and Song, 2023). A study by Kurian et al, found that Al-pillared bentonite catalysts enhance gasification efficiency by increasing the H₂/CO ratio and reducing tar content by up to 40% (Kurian and Kavitha, 2016).

Research published in Fuel (2020) discusses the impact of Fe metal catalysts on lignocellulosic gasification, reporting a 30% increase in thermal efficiency (Lu et al., 2020). Kwon et al, demonstrated the effectiveness of metal-pillared bentonite in catalytic reforming processes, extending catalyst life and improving syngas synthesis efficiency by 25% (Kwon et al., 2024).

However, despite numerous studies on bentonite- or transition metal-based catalysts, no research specifically examines the use of Al-Fe metal-pillared bentonite catalysts in the gasification of EFB and palm kernel shell waste. Additionally, the effects of acid activation and metal pillaring on gasification parameters, such as syngas volume, %NGC, %GC, and energy quality (e.g., %HHV and %LHV), are still very limited in the literature. Therefore, this study focuses on developing Al/Fe metal-pillared bentonite catalysts to improve the gasification efficiency of palm kernel shell. This study aims to synthesize Al/Fe metal-pillared bentonite catalysts through acid activation and metal pillaring, and to evaluate their performance in palm kernel shell gasification using FTIR, XRD, SEM, and EDS characterization.

The study will then analyze syngas volume, %NGC, %GC, %HHV, %LHV, %CCE, and %CGE to assess the practical potential of Al/Fe metal-pillared bentonite catalysts in biomass gasification processes.

MATERIALS AND METHODS

Materials

The natural bentonite used in this study was technical-grade bentonite powder obtained from a local supplier as the base material. Sulfuric acid (H₂SO₄) was used as the activation solution, while Al and Fe were used as the pillaring metals. A 5% NaOH solution was employed to dissolve the aluminum and iron metals. Distilled water (aquadest) was used as the washing and rinsing medium throughout all stages of the process.

Synthesis of the Al/Fe metal-pillared bentonite catalyst

The preparation of the metal-pillared bentonite catalyst began with the activation of bentonite. A total of 5 grams of technical-grade bentonite powder was weighed and activated by treating it with 200 ml of a 5% sulfuric acid (H₂SO₄)

solution. The activation process was carried out for 8 hours to enhance the surface area and increase the adsorption capacity of the bentonite. After activation, the bentonite was thoroughly washed and centrifuged to achieve a neutral pH. Following the washing process, the bentonite was dried in an oven at 80 °C for 1 hour, and then sieved using a mesh size of 100 to obtain a uniform particle size for further analysis.

To prepare the metal solutions, Al and Fe were each dissolved in 240 ml of a 5% sodium hydroxide (NaOH) solution. These metal solutions were mixed for 2 hours and allowed to stand at room temperature for 2 days. This process facilitated the formation of metal ions, which would later be used in the pillaring process.

The next step involved combining the activated bentonite with the prepared metal solutions. The mixture was blended at a speed of 1000 rpm for 24 hours at room temperature. After blending, the mixture was filtered to remove excess liquid, and then dried in an oven at 80 °C for 1 hour. The dried product was sieved again using a mesh size of 100 to ensure a consistent particle size.

Finally, the bentonite-metal mixture underwent calcination at a temperature of 400 °C for 2 hours. This calcination step was crucial for stabilizing the metal pillars within the bentonite structure and enhancing its catalytic properties (Figure 1).

Characterization of the Al/Fe metal-pillared bentonite catalyst

Characterization was performed to study the structural changes and improvements in

physicochemical properties after modification. FT-IR analysis was conducted using the Thermo Scientific Nicolet iS10 FTIR spectrometer, located at the Faculty of Mathematics and Natural Sciences Laboratory, Sriwijaya University, to identify functional groups and structural modifications in the catalyst. SEM-EDS measurements were carried out to analyze the surface morphology and elemental composition of the metal-pillared bentonite, following the ASTM D7582 standard, at the Faculty of Engineering Laboratory, Sriwijaya University.

Application of the Al/Fe metal-pillared bentonite catalyst in biomass gasification

The catalytic gasification of empty fruit bunches (EFB) was carried out using a fixed-bed updraft gasifier with 5 kg of EFB. Metal-pillared bentonite catalysts (Al and Fe) were tested at concentrations of 1.25% and 2.50%. These concentrations were selected based on preliminary studies, which indicated optimal catalytic performance in reducing tar and enhancing syngas yield. The gasifier operated at a temperature of 550°C, with an air-oxygen mixture as the gasifying agent at a flow rate of 10 liters per minute. During the gasification process, EFB is converted into synthesis gas (syngas), consisting of hydrogen (H₂), carbon monoxide (CO), methane (CH₄), and other hydrocarbons. The metal-pillared bentonite catalyst enhances efficiency by improving thermal stability and catalytic activity, reducing tar formation, and increasing gasification yields.



Figure 1. Catalyst materials: (a) natural bentonite, (b) activated bentonite, and (c) metal-pillared bentonite

Analysis data

In the analysis of FTIR, SEM-EDS, and XRD data, OriginPro is used to process and analyze spectral data as well as experimental images. The experimental data is imported into the software. Then, OriginPro is used to identify peaks in the FTIR spectrum that represent functional groups, as well as to analyze morphology, 3D images, and catalyst porosity from the SEM-EDS data. For XRD data, OriginPro helps identify diffraction peaks, determine crystal phases, and calculate crystallographic parameters. Using features like Peak Analyzer and Image Analysis, the data is processed and visualized to facilitate the interpretation and analysis of the research results. The crystal size from X-ray diffraction (XRD) data is calculated using the Scherrer equation:

$$D = \frac{K\lambda}{\beta \cdot \cos\theta} \quad (1)$$

where: D is the crystal size (nm), K is the Scherrer constant, λ is the X-ray wavelength (nm), β is the full width at half maximum (FWHM) of the diffraction peak in radians, θ is the Bragg angle (half of 2θ) in radians.

The percentage of crystallinity (C% C%) in materials can be calculated using XRD data through the peak area approach. The formula is:

$$\%C = \frac{CP}{AT \text{ (amorphous + crystalline)}} \times 100\% \quad (2)$$

where: CP – crystalline peaks, AT – area total

The gas composition analysis in this study was conducted using gas chromatography to identify the main components of the produced syngas, such as hydrogen (H_2), carbon monoxide (CO), methane (CH_4), and carbon dioxide (CO_2). After analyzing the gas composition, the gasification process efficiency was calculated using several key parameters.

Gas conversion efficiency (%GC) measures the efficiency of converting biomass into gas and is calculated using the formula:

$$\%GC = \left(\frac{\text{Gas Volume}}{\text{Biomass Volume}} \right) \times 100 \quad (3)$$

The higher the %GC, the better the conversion of biomass into syngas. Non-gas conversion efficiency (%NGC) measures the amount of biomass that is not converted into gas, and it is calculated using the formula:

$$\%NGC = 100 - \%GC \quad (4)$$

HHV is used to calculate the maximum energy produced, while LHV provides a more realistic

measure of the energy that can be practically used. The formula for calculating the higher heating value (HHV) of a fuel is:

$$HHV = \sum HF_i \times \sum MF_i \quad (5)$$

where: HF_i is the heating value of each component (e.g., H_2 , C, CH_4), MF_i is the molar fraction of each component in the fuel.

The general formula for calculating the lower heating value (LHV) is:

$$LHV = HHV - (h_{\text{vapor}} \times MWP) \quad (6)$$

where: HHV is the higher heating value, h_{xxx} is the latent heat of vaporization of water, Mass of water produced refers to the amount of water produced during the combustion of the fuel.

Carbon conversion efficiency (%CEE) calculates the efficiency of converting carbon in biomass into gases like CO and H_2 , using the formula:

$$\%CEE = \left(\frac{\text{Carbon in Gas}}{\text{Carbon in Biomass}} \right) \times 100 \quad (7)$$

where: *Carbon in gas* refers to the amount of carbon present in the gas products (e.g., CO, H_2). *Carbon in biomass* is the total amount of carbon initially present in the biomass feedstock.

Cold gas efficiency (%CGE) measures the energy efficiency of syngas produced at low temperatures, calculated using the formula:

$$\%CGE = \left(\frac{\text{Energy in Syngas}}{\text{Energy in Biomass}} \right) \times 100 \quad (8)$$

where: *Energy in syngas* is the total energy content of the produced syngas (syngas heating value), *Energy in biomass* is the total energy content of the biomass feedstock.

RESULT AND DISCUSSION

Synthesis of Al/Fe-pillared bentonite catalyst

The synthesis process of Al/Fe-pillared bentonite catalyst begins with the activation of natural bentonite using sulfuric acid (H_2SO_4). This activation aims to enhance the ion exchange capacity and open the interlayer structure of the bentonite. Afterward, the bentonite is intercalated with Al/Fe polymeric cations formed through the reaction of metal precursors with a base. The final product is a powder of Al/Fe-pillared bentonite with improved thermal, structural, and catalytic properties. Below is a detailed explanation of the reaction steps:

- Activation reaction :
 $Bentonite-Na + H_2SO_4 \rightarrow Bentonite-H + Na_2SO_4(9)$

- Formation of Aluminium Pillar Cations:
 $AlCl_3 + 3NaOH \rightarrow Al(OH)_3 + 3NaCl \quad (10)$

 $13Al(OH)_3 + 4OH^- \rightarrow [Al_{13}O_4(OH)_{24}]^{7+} + 12H_2O(11)$

- Formation of Iron Pillar Cations:
 $FeCl_3 + 3NaOH \rightarrow Fe(OH)_3 + 3NaCl \quad (12)$

 $xFe(OH)_3 \rightarrow [Fe_x(OH)_y]^{3x-y} \quad (13)$

Characterization of Al/Fe-pillared bentonite catalyst

The characterization was conducted using FTIR, SEM-EDS, and XRD analyses on three samples: natural bentonite, acid-activated bentonite, and metal-pillared bentonite. This study aims to compare the differences in structure, composition, and physicochemical properties of the three samples and identify the changes resulting from acid activation and metal pillaring. The analysis results are explained as follows.

FTIR analysis

FTIR analysis was conducted to determine the chemical components of the catalyst. The peaks in the spectrum provide information about functional bonds, which help evaluate the material’s characteristics and its potential applications. The samples used were natural bentonite, acid-activated

bentonite, and metal-pillared bentonite. The analysis results are shown in Figure 2, with the FTIR graph displaying the wavenumber (cm⁻¹) on the X-axis and absorbance intensity on the Y-axis.

The FTIR spectrum in the Figure 2 shows significant structural changes in natural bentonite, acid-activated bentonite, and metal-pillared bentonite, reflecting modifications to their physicochemical properties. Natural bentonite exhibits a characteristic peak around 3451 cm⁻¹, associated with O-H stretching vibrations from hydroxyl groups, and a peak at 1637 cm⁻¹, corresponding to asymmetric stretching of bound water. The region between 797–1035 cm⁻¹ reveals Si-O-Si and Al-O-Si vibrations, indicating the basic montmorillonite framework without chemical treatment. However, this structure limits active surface area and reactive sites, reducing catalytic efficiency, as noted by (Ihekweze et al., 2020).

In acid-activated bentonite, the intensity of the -OH peak at 3451 cm⁻¹ decreases, signifying the partial removal of interlayer water. The disappearance of peaks in the 2000–2500 cm⁻¹ region indicates the dissolution of interlayer cations, while changes at 1637 cm⁻¹ confirm partial dehydration. These modifications increase specific surface area and active sites, enhancing its adsorption properties. Wang et al., reported that acid activation generates a more amorphous structure with improved adsorption capacity, making it suitable for industrial and environmental applications (Wang et al., 2023).

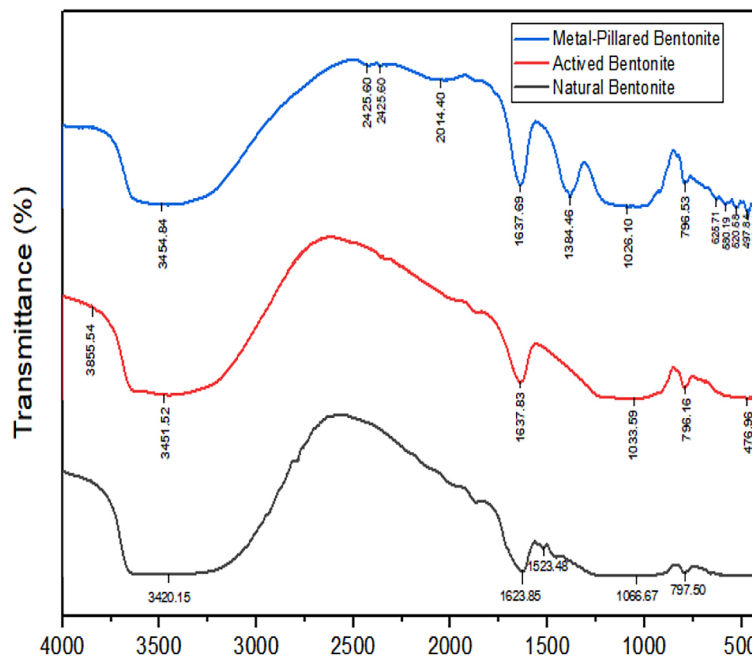


Figure 2. FTIR spectrum of the catalyst: natural, activated, and metal-pillared bentonite

The metal-pillared bentonite spectrum reveals new peaks around $1423\text{--}1065\text{ cm}^{-1}$, indicative of metal-O group formation due to the pillaring process with Al and Fe. The reduced intensity of the O-H stretching peak at 3451 cm^{-1} reflects interactions between the metal and surface hydroxyl groups. These structural changes enhance stability, adsorption capacity, and suitability for heterogeneous catalysis. According to Liu et al., Al- and Fe-pillared bentonite demonstrates superior performance in wastewater treatment and catalytic applications (Liu et al., 2024).

In conclusion, modifications via acid activation and metal pillaring significantly improve bentonite's catalytic properties, making it highly effective for biomass gasification and other advanced applications. Studies by Maitlo et al., highlight that Fe/Al-pillared catalysts not only increase syngas yields but also lower operational temperatures, underscoring their industrial relevance (Maitlo et al., 2022).

SEM image analysis

Scanning electron microscopy (SEM) analysis was conducted to identify and understand the elemental composition of natural bentonite samples. This approach provides essential information regarding the elemental distribution and microstructural characteristics that influence the physical and chemical properties of the material. Figures 3 show SEM images of the surface of natural bentonite, activated bentonite, and metal-pillared bentonite at a magnification of 1200x.

Figure 3a shows an SEM image of natural bentonite with a rough and irregular surface, containing micro-sized particles. This structure indicates that bentonite possesses natural porosity, which is important for adsorption applications.

The porous surface provides a large area for interactions with molecules or ions. This finding is supported by research from Mane et al, which shows that porous surfaces offer space for metal ions (Mane et al., 2024).

Figure 3b shows an SEM image of bentonite activated with sulfuric acid, which has a smoother surface with wider pores. Acid activation enhances the porosity and surface area of bentonite, increasing its adsorption capacity. Ibigbami et al., found that acid-activated bentonite is effective in removing heavy metals from wastewater, improving the adsorption of Zn, Ni, and Fe. Additionally, Berhe et al., demonstrated that acid-activated bentonite has high catalytic activity due to the presence of acid sites that accelerate reactions (Berhe et al., 2024)

Figure 3c shows an SEM image of bentonite pillared with Al and Fe, which has a denser and more uniform surface compared to natural or acid-activated bentonite. This surface is rough, with fine porous layers, indicating more active sites. The pillaring process enhances the thermal stability and surface area of bentonite, making it more effective for adsorption and catalytic applications. Studies have shown that Fe- and Al-pillared bentonite exhibit high catalytic activity in processes such as biomass gasification and organic pollutant degradation (Vallejo et al., 2020).

3D image of bentonite catalyst

The 3D image of the bentonite catalyst, obtained through acid activation and metal pillaring, illustrates the X, Y, and Z axes as the components defining the spatial structure. These axes represent the width, height, and depth of the catalyst, providing a comprehensive view of its surface morphology and structural modifications. In this 3D visualization, solid spaces are observed,

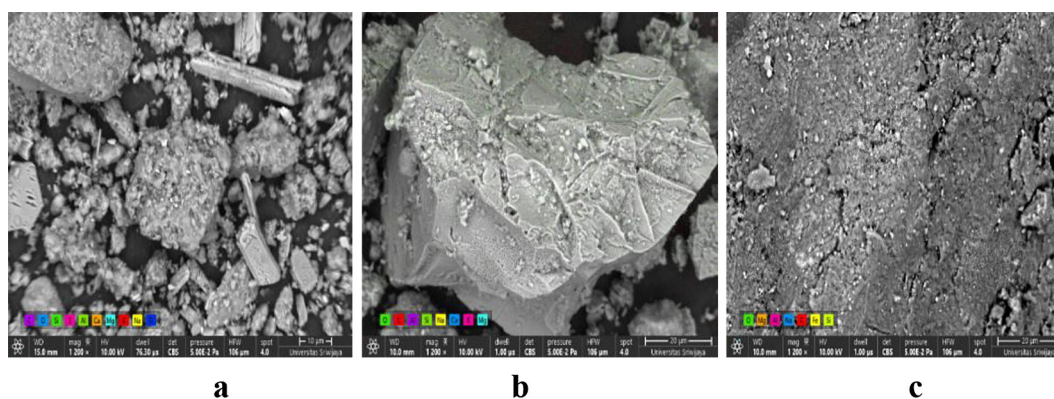


Figure 3. SEM image of the catalyst: (a) natural bentonite, (b) activated bentonite, (c) metal-pillared bentonite

representing the dense material structure, as well as pore spaces, indicating void areas within the material that play a crucial role in its porosity and adsorption capacity. The distinction between solid and pore spaces highlights the enhanced porosity resulting from acid activation and metal pillaring, offering valuable insights into the catalyst's potential applications, particularly in processes requiring high surface area and improved adsorption or catalytic properties. The 3D catalyst images are shown in Figure 4.

Figure 4a The natural bentonite catalyst exhibits a structure with large and irregularly distributed particles, reflecting its natural form without significant modification. This structure results in a low specific surface area, limiting its capability in applications requiring high interaction with molecules, such as catalysis or adsorption. Therefore, natural bentonite is more suitable as a base material that requires further modification to enhance its effectiveness in practical applications. Research by Amari et al, supports this observation, demonstrating that while natural bentonite has adsorption potential, its ability to remove pollutants is limited due to its larger and less organized particle structure (Amari et al., 2021).

Figure 4b Acid-activated bentonite shows significant changes in particle morphology, with smoother surfaces and increased porosity due to the removal of mineral impurities during the acid activation process. This activation creates more pore spaces and additional active sites, which are beneficial for adsorption and catalytic processes. Acid activation, typically performed using H_2SO_4 or HNO_3 , has been shown to enhance the adsorption capacity of the material for heavy metals and organic compounds. Acid-activated bentonite demonstrates higher adsorption efficiency, as evidenced by Taghavi et al, who reported an improvement of over 85% in removing organic pollutants and heavy metals (Taghavi et al., 2022).

Figure 4c metal-pillared bentonite exhibits a more organized structure with uniform pore distribution due to the introduction of metal pillars such as Al and Fe. This process creates a layered structure that not only enhances mechanical and thermal stability but also adds catalytic active sites. These metal pillars play a critical role in catalytic applications, such as biomass gasification and Fenton reactions, by improving reaction efficiency through better diffusion pathways for reactants. Research by Bellucci et al. (2023)

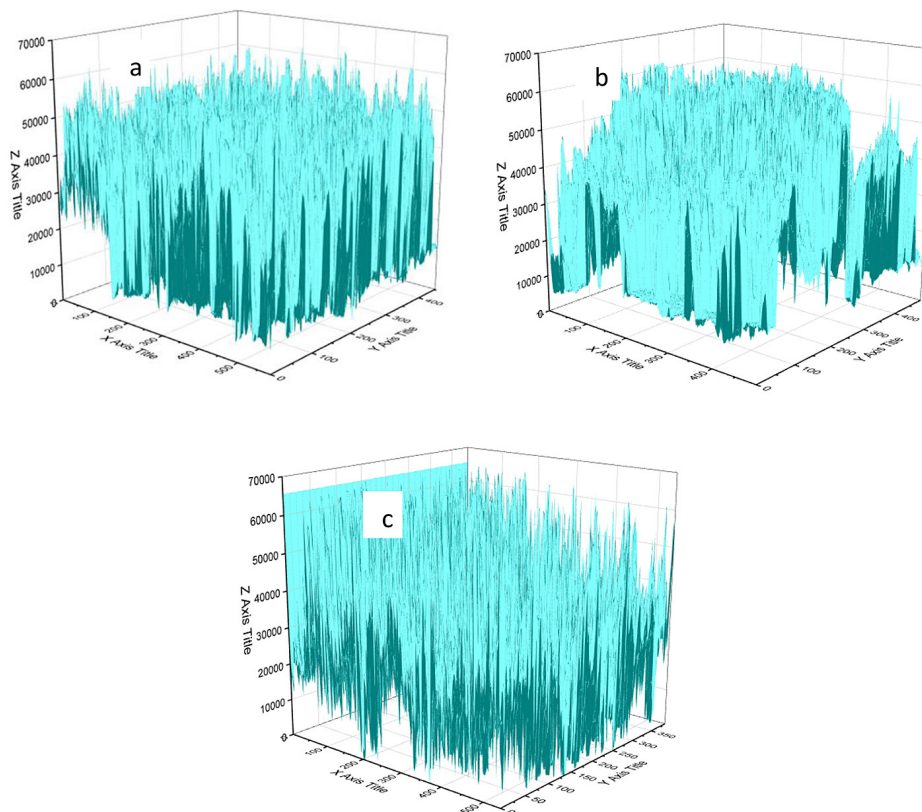


Figure 4. 3D image of catalysts: (a) natural bentonite, (b) acid-activated bentonite, and (c) Al/Fe metal-pillared bentonite

indicates that metal-pillared bentonite significantly improves adsorption capacity and catalytic activity compared to natural and acid-activated bentonite.

Porosity analysis of the catalyst

The quantitative analysis of three types of bentonite catalysts, namely natural bentonite, acid-activated bentonite, and metal-pillared bentonite (Al/Fe), shows significant changes in porosity and microstructure properties. The data on the porosity percentage and catalyst volume are presented in Table 1.

Table 1 shows that natural bentonite catalyst has a porosity of 54.44% and a total pore volume of $1.348 \times 10^{-20} \text{ m}^3$. The natural structure of bentonite consists of large, unmodified particles, with an uneven pore distribution. Despite its high porosity, the majority of the volume is occupied by solid components ($1.127 \times 10^{-20} \text{ m}^3$), indicating that this material is not yet optimized for catalytic or adsorption applications. Natural bentonite is more suitable as a base material for further modification. Recent studies have shown that raw bentonite, although having adsorption potential, requires further treatment to improve its surface properties. For example, research by Khalfaoui et al. (2019) demonstrated that raw bentonite has limited heavy metal adsorption capacity compared to after activation.

The acid activation process results in a bentonite catalyst with a porosity of 50.81% and a pore volume of $4.431 \times 10^{-21} \text{ m}^3$, which is lower

than that of natural bentonite. This decrease in porosity is compensated by an increase in the number of active sites and micropores. Acid activation removes impurities such as carbonates or metal oxides, enhancing the chemical interaction at the surface. The solid volume decreases to $4.290 \times 10^{-21} \text{ m}^3$, indicating a more efficient acid modification. Research by Wang et al. (2021) demonstrated that activation with H_2SO_4 increases the adsorption efficiency of organic dyes by up to 80%, proving that the adsorption and catalytic properties of acid-activated bentonite heavily depend on the improvement of its surface microstructure. Additionally, other studies have shown that acid treatment improves the interaction of ions with the bentonite surface, making it more chemically active for environmental applications.

Metal pillaring with Al/Fe results in a bentonite catalyst with a porosity of 54.36% and a pore volume of $7.448 \times 10^{-21} \text{ m}^3$, which is higher than that of acid-activated bentonite. The increase in pore volume indicates the success of pillaring in creating a more open and organized structure. The larger solid volume ($6.256 \times 10^{-21} \text{ m}^3$) reflects the contribution of metal pillars that enhance the stability of the material. This structure is highly effective for heterogeneous catalyst applications, such as biomass gasification. Research by Liu et al. (2022) showed that iron-pillar bentonite increased catalytic reactivity by up to 65% in the Fenton oxidation reaction, as the metal pillars enhance surface area and availability of active sites. Moreover, the thermal stability of metal-pillared

Table 1. Porosity percentage and catalyst volume

Material	Parameter	Value	Unit
Natural bentonite	Solid volume (V solid)	2.475×10^{-20}	m^3
	Solid volume (V solid)	1.127×10^{-20}	m^3
	Pore volume (V pori)	1.348×10^{-20}	m^3
	Porosity porositas	0.54	-
	Porosity percentage	54.44	%
Acid-activated bentonite	Solid volume (V solid)	8.722×10^{-21}	m^3
	Solid volume (V solid)	4.290×10^{-21}	m^3
	Pore volume (V pori)	4.431×10^{-21}	m^3
	Porosity	0.51	-
	Porosity percentage	50.8	%
Metal-pillared bentonite	Solid volume (V solid)	1.370×10^{-20}	m^3
	Solid volume (V solid)	6.256×10^{-21}	m^3
	Pore volume (V pori)	7.448×10^{-21}	m^3
	Porosity	0.54	-
	Porosity percentage	54.36	%

bentonite is higher, making it ideal for high-temperature applications such as gasification.

Chemical treatments such as acid activation and metal pillaring affect the porosity properties and pore volume distribution of bentonite. Natural bentonite has high porosity but is not yet effective for certain applications. Acid activation enhances active sites, making it suitable for adsorption, while metal-pillared bentonite exhibits a stable structure with large pores, making it superior for catalytic applications, particularly in biomass gasification.

EDS analysis

The energy dispersive (EDS) X-ray analysis was used to identify the elemental composition of natural bentonite, activated bentonite, and pillared bentonite. The EDS spectra show the distribution of key elements such as O, Si, and Al, which are the main components in the bentonite structure. Changes in the intensity of certain elements in activated and pillared bentonite reflect chemical modifications during the activation and pillaring processes. The data in Table 2 help evaluate the material property changes under different treatments.

The EDS analysis results presented in provide insights into the chemical composition changes of natural bentonite, activated bentonite, and metal-pillared bentonite. In natural bentonite, the dominance of oxygen (48.5% wt.) and silicon (24.1% wt.) indicates the fundamental structure of bentonite, which consists of silica and alumina layers. The presence of aluminum (4.4% wt.) as a key component highlights the aluminosilicate character of bentonite. The

relatively high carbon content (21.3% wt.) suggests the possibility of organic contamination, which is common in raw bentonite, as explained by Keereerak et al. (2022). This structure reflects the inherent characteristics of bentonite as an unmodified natural mineral material.

For activated bentonite, the EDS results show an increase in oxygen content (50.8% wt.) and a decrease in carbon content (11.2% wt.), indicating the removal of organic contaminants through acid activation. This activation also increases aluminum (7.8% wt.) and silicon (24.0% wt.) content, suggesting a restructuring of the aluminosilicate framework. The higher oxygen content reflects the formation of additional hydroxyl (OH) groups, enhancing the adsorption capability of the bentonite, as supported by studies by Crespo et al., 2024 and Liu et al., 2019. This process involves the dissolution of certain components, resulting in a larger active surface area and improved adsorptive properties.

In metal-pillared bentonite, oxygen remains the dominant element (49.5% wt.), but a significant increase in aluminum (12.9% wt.) and the appearance of iron (8.0% wt.) indicate the successful incorporation of metal pillars. These metal pillars, such as Al and Fe, stabilize the bentonite structure while increasing its active surface area. The presence of iron significantly contributes to the catalytic properties of bentonite, making it suitable for oxidation reactions, as confirmed by Vallejo et al. (2020). The increased metal content, particularly Fe, enhances the catalytic ability of bentonite for the decomposition of organic compounds, which is a critical factor in heterogeneous catalysis.

Table 2. Elemental composition of catalyst

Element	Natural bentonite		Activated bentonite		Metal-pillared bentonite	
	At. %	Wt. %	At. %	Wt. %	At. %	Wt. %
C	21.3	14	17	11.2	3.6	2.1
O	55.3	48.5	58.2	50.8	63.1	49.5
Na	0.3	0.4	1.8	2.2	2.1	2.4
Mg	0.6	0.9	0.3	0.3	1.7	2
Al	3	4.4	5.3	7.8	9.8	12.9
Si	15.7	24.1	15.7	24	16.8	23.1
S	1.4	2.4	-	-	-	-
K	0.4	0.8	0.6	1.2	-	-
Ca	1.7	3.8	1.1	2.5	-	-
Ti	0.3	0.7	-	-	-	-
Fe	-	-	-	-	2.9	8

X-ray diffraction pattern

XRD is a technique used to analyze changes in the crystal structure of materials. The comparison of diffraction peak intensities and positions (2θ) reveals variations in crystallinity, layer structures, and the distribution of mineral phases within the materials. These insights are crucial for assessing the effectiveness of modifications on material properties, particularly for their use as catalysts in biomass gasification. The X-ray diffraction pattern for bentonite catalysts is shown in the Figure 5.

Figure 5 presents the XRD results for natural, activated, and metal-pillared bentonite, highlighting significant crystal structure transformations due to modification treatments. The natural bentonite (black line) exhibits broad, low-intensity peaks at 2θ around $20\text{--}25^\circ$, indicating an amorphous structure with low crystallinity. The activated bentonite (red line) shows sharper peaks at 2θ values of 26° and 36° , reflecting increased crystallinity from chemical activation, commonly acid treatment, which removes impurities and enhances adsorption properties. This observation aligns with findings by (Wei et al., 2020).

The metal-pillared bentonite (blue line) features the sharpest and most intense peaks, notably at 2θ values of 18° , 27° , and 60° , confirming successful intercalation of metals such as Al or Fe into montmorillonite layers. This process enhances

structural order, creating mesoporous material with superior thermal stability and adsorption capacity. Studies by Cuevas et al. (2022) report similar results, with sharp peaks at 27° as a key indicator of modification success.

The observed structural transformation affirms the effectiveness of these modifications, positioning these materials as excellent candidates for catalysts in biomass gasification applications.

Catalyst crystal size

The crystal size provides insight into the effects of activation and pillaring processes on the crystal structure of bentonite. The average crystal size of the catalyst was calculated using the Equation 1. The results of the calculation are presented in Table 3.

The crystal size of bentonite materials is crucial for their effectiveness as catalysts in biomass gasification, as it affects factors such as surface area, thermal stability, and the number of active sites that speed up reactions. According to Table 3, natural bentonite, with a crystal size of 5.260 nm, has a

Table 3. Crystal size of different types of catalysts

Material	Average crystal size
Natural bentonite	5.26
Activated bentonite	4.896
Metal pillared bentonite	22.152

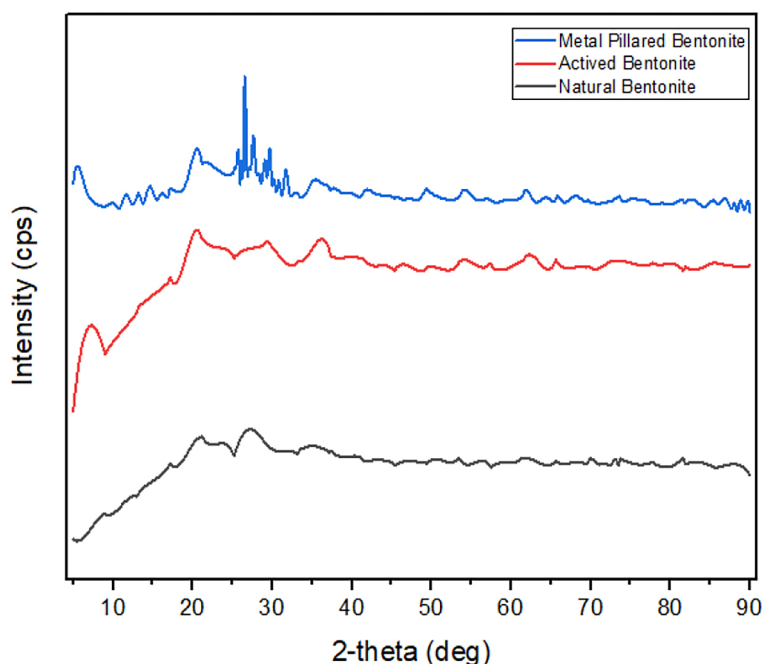


Figure 5. X-ray diffraction patterns for natural, activated, and metal-pillared bentonite

relatively large surface area but limited catalytic activity due to its low crystallinity and amorphous structure, making it suitable for further development. Activated bentonite, with a smaller crystal size of 4.896 nm, shows improved crystallinity and more active sites, enhancing its catalytic efficiency. This is consistent with Gandhi et al., who found that chemical activation (using acid or base) increases crystallinity and surface area, improving the catalytic and adsorption properties of bentonite (Gandhi et al., 2022). Metal-pillared bentonite, with the largest crystal size of 22.152 nm, offers excellent thermal stability and mechanical strength due to metal intercalation, forming a mesoporous structure. Although it has a smaller surface area compared to activated bentonite, it is more efficient in reducing tar and increasing hydrogen production at high temperatures (500–900 °C), as shown by (Nganda et al., 2023). These results highlight the importance of crystal size and modifications like activation and metal-pillaring for optimizing bentonite’s catalytic potential in biomass gasification.

Percentage of crystallinity

The crystallinity percentage of various catalysts was analyzed to evaluate the effect of modification processes on their structural properties. The percentage of the catalyst crystallinity was calculated using Equation 2. The results of the analysis are presented in Table 4.

The crystallinity percentage (% C) of bentonite plays an important role in its physical and chemical properties, especially for catalytic applications like biomass gasification. According to Table 4, natural bentonite has a crystallinity of 66.21%, indicating a stable structure dominated by montmorillonite. This structure gives it good stability but is not ideal for catalytic use without modification.

In activated bentonite, the crystallinity decreases to 54.75% due to disruptions in the crystal structure during activation, such as impurity removal and pore opening. Despite the lower crystallinity, this increases the surface area and number of active sites, making it more effective in catalytic and adsorption applications.

Table 4. Crystallinity percentage of different catalysts

Material	Crystallinity percentage (%C)
Natural bentonite	66.21
Activated bentonite	54.75
Metal pillared bentonite	68.96

Metal-pillared bentonite has the highest crystallinity at 68.96%, showing that the intercalation of metals like Al or Fe improves the crystal structure, stability, and catalytic capacity. The mesoporous structure created is ideal for high-temperature applications like biomass gasification, where stability and efficiency are critical.

In summary, changes in crystallinity highlight the effects of modification processes on bentonite, making it more suitable for various catalytic applications.

The effect of catalysts on the gas composition of EFB gasification

The use of catalysts in the gasification process has been proven to significantly influence the composition of the resulting gas, particularly by enhancing the production of high-calorific-value gases such as hydrogen (H₂) and carbon monoxide (CO). In this study, the effect of catalysts on the gas composition produced from the gasification of empty palm fruit bunches was analyzed to understand the role of catalysts in optimizing the key chemical reactions during the process. The gas composition from the GC analysis is presented in Figure 6.

The analysis of the data in the Figure 6 demonstrates that the use of catalysts plays a crucial role in enhancing the gas composition produced during the gasification of EFB, especially in increasing the concentrations of combustible gases such as hydrogen (H₂), carbon monoxide (CO), and methane (CH₄), while reducing the presence of non-combustible gases like carbon dioxide (CO₂) and inert gases. Without a catalyst, H₂ concentration is

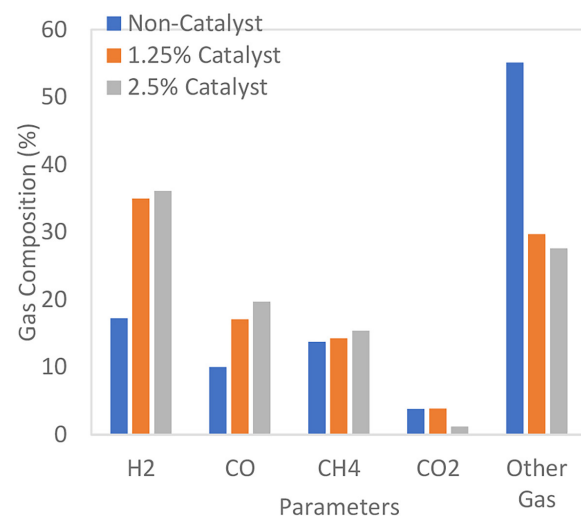


Figure 6. Gas composition of empty fruit bunches

at its lowest (17.27%), but it significantly increases to 35% with 1.25% catalyst and further to 36.1% with 2.5% catalyst. This improvement is attributed to the accelerated water-gas shift reaction ($\text{CO} + \text{H}_2\text{O} \rightarrow \text{CO}_2 + \text{H}_2$), where catalysts enhance the production of H_2 , a high-energy gas.

Similarly, CO concentration increases from 10.02% in non-catalytic conditions to 17.1% with 1.25% catalyst and peaks at 19.7% with 2.5% catalyst. This reflects the enhanced decomposition of carbon in biomass and the Boudouard reaction ($\text{C} + \text{CO}_2 \rightarrow 2\text{CO}$), although some CO is converted into H_2 via the water-gas shift reaction. Methane (CH_4) shows a modest increase, rising from 13.75% without a catalyst to 14.2% with 1.25% catalyst and 15.4% with 2.5% catalyst. This is linked to the reforming of hydrocarbons into lighter, energy-dense gases.

On the other hand, CO_2 concentration decreases with the addition of catalysts, from 3.82% in non-catalytic conditions to 1.2% with 2.5% catalyst. This reduction indicates the efficiency of the catalyst in redirecting carbon from CO_2 to produce CO and H_2 . Moreover, inert gases, which dominate the gas composition in non-catalytic conditions (55.14%), are reduced significantly to 29.73% with 1.25% catalyst and further to 27.6% with 2.5% catalyst. This decrease underscores the ability of catalysts to minimize non-useful gas formation and enhance the production of energy-rich gases.

Recent studies validate these findings. Ebrahimi et al., demonstrated that metal-based catalysts enhance H_2 production via water-gas shift reactions (Ebrahimi et al., 2020). Similarly, Adadullah et al, found that catalysts improve gasification energy efficiency by up to 20% (Asadullah et al., 2004). Wang et al, also observed reduced CO_2 and inert gas formation with catalysts, resulting in improved gasification performance (Wang et al., 2020).

Overall, the addition of catalysts, particularly at a concentration of 2.5%, significantly improves the gasification process by increasing the yield of combustible gases like H_2 and CO while reducing CO_2 and inert gases, making it an effective strategy to produce high-quality syngas with better energy potential.

The effect of catalyst on process efficiency

The ratio of combustible gas to non-combustible gas shows the comparison between combustible and non-combustible gases produced during the gasification process. This ratio is important

for evaluating the gasification efficiency of fuels, such as biomass and palm shell, in energy production. Combustible gases include H_2 , CH_4 , and CO, while non-combustible gases include CO_2 and N_2 . A higher ratio indicates better gasification efficiency, as it means more combustible gases are produced, which increases energy potential. The GC and NGC values are calculated using Equation 3 and Equation 4 and are shown in Figure 7.

The analysis of biomass gasification efficiency shown in Figure 7 highlights the significant impact of catalysts on improving performance. The use of catalysts increases the production of GC, reduces NGC, and improves the GC/NGC ratio. Without a catalyst, GC was 41.04%, with a GC/NGC ratio of 0.696. With 1.25% and 2.5% catalysts, GC increased to 66.4% and 71.2%, and the GC/NGC ratios rose to 1.976 and 2.472, respectively. NGC dropped from 58.96% to 33.6% (1.25% catalyst) and 28.8% (2.5% catalyst), showing that catalysts not only enhance high-energy gas formation but also reduce low-energy gas production.

This improvement is due to catalytic mechanisms that accelerate reforming, decomposition, and water-gas shift reactions, increasing the production of H_2 and CO. A study by Maitlo et al. (2022), reported that metal-based catalysts enhance biomass gasification efficiency, maximizing high-quality syngas production. Additionally, research published showed that nickel-cerium catalysts improve hydrogen production efficiency by up to 50% by reducing tar and inert gas formation, aligning with this study's findings (Yuan et al., 2022).

These results emphasize the importance of catalysts, especially at 2.5%, in optimizing gasification

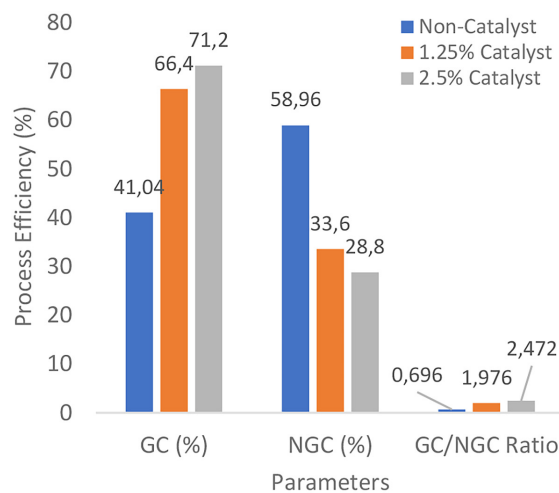


Figure 7. Process efficiency of GC/NGC

efficiency. By reducing non-reactive gases and increasing reactive ones, catalytic biomass gasification contributes to cleaner and more sustainable energy production, highlighting the need for further research in advanced catalyst development.

The effect of catalysts on heating value of EFB gasification processes

The heating value refers to the amount of energy released during the combustion of a fuel. There are two main categories: higher heating value (HHV) and lower heating value (LHV). HHV includes the total energy released, including energy from the water vapor produced, while LHV does not account for this energy, assuming the water vapor does not condense. HHV is used to calculate the maximum energy that can be produced, while LHV provides a more realistic measure of energy available for practical use. The HHV and LHV values from the TKKS gasification process are calculated using Equation 5 and Equation 6, and the results are presented in Figure 8.

Figure 8 shows the HHV and LHV of gas produced from the gasification of EFB with and without catalysts, highlighting the positive effect of aluminum-based catalysts on energy quality. Without a catalyst, the HHV is 8.94 MJ/Nm³. With 1.25% catalyst, HHV increases to 12.32 MJ/Nm³, and with 2.5% catalyst, it rises further to 13.22 MJ/Nm³. Similarly, the LHV starts at 7.39 MJ/Nm³ without a catalyst, increases to 9.17 MJ/Nm³ with 1.25% catalyst, and reaches 9.97 MJ/Nm³ with 2.5% catalyst. These improvements show that the catalyst enhances the gas’s energy content and the overall gasification efficiency, producing gas better

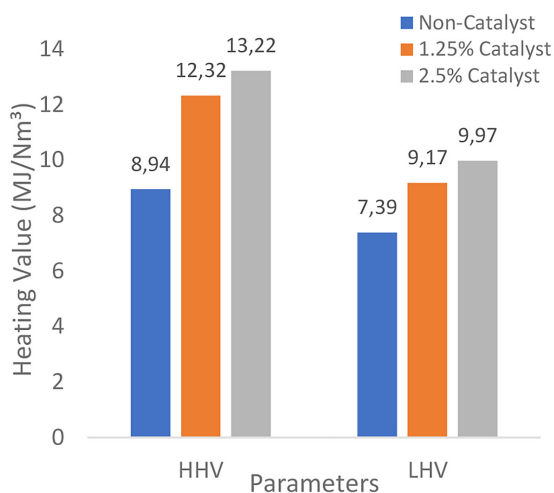


Figure 8. Heating value of EFB

suited for combustion and energy generation. Recent studies confirm that catalysts, especially aluminum-based ones, increase the HHV and LHV of syngas by accelerating the conversion of biomass into high-quality syngas (Wu et al., 2023).

The effect of catalysts on gasification efficiency of EFB gasification processes

Cold gas efficiency (CCE) and cold gasification efficiency (CGE) are two parameters used to measure the efficiency of biomass gasification processes. These parameters provide an overview of how efficiently biomass can be converted into useful gases for energy production. Higher CCE and CGE values indicate a more efficient gasification process in producing usable gases. The percentage of CCE and CGE are calculated using Equation 7 and Equation 8, and the results are presented in Figure 9.

The Figure 9 showing %CCE and %CGE demonstrates that the addition of aluminum-based catalysts significantly improves the efficiency of the gasification process of EFB. The %CCE without a catalyst is recorded at 62.70%, which increases to 80.16% with 1.25% catalyst and reaches 82.50% with 2.5% catalyst. This improvement indicates that the catalyst helps enhance the amount of usable gas in a cold state, making the process more efficient.

Meanwhile, %CGE without a catalyst is 27.86%, which increases to 38.37% with 1.25% catalyst and 41.19% with 2.5% catalyst. This suggests that the catalyst also contributes to increasing the ratio of energy that can be

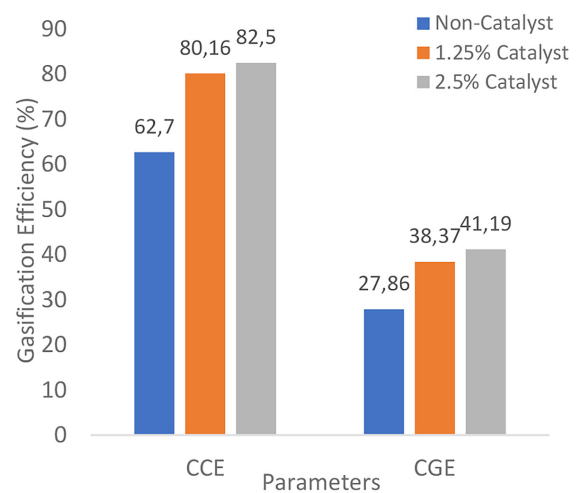


Figure 9. Gasification efficiency

recovered from the gasification process, resulting in more usable energy.

The use of catalysts in biomass gasification, especially for materials like EFB, has been shown to significantly improve process efficiency, both in terms of CCE and CGE. The results obtained show significant improvements in both parameters, with the 2.5% catalyst yielding the best results, increasing energy efficiency and reducing tar formation. Research by Gao et al. (2020) shows that modified olivine catalysts with metals such as nickel and cerium can improve hydrogen production, reduce methane, and enhance syngas quality (Gao et al., 2021). Catalysts also help reduce tar formation, which can hinder downstream efficiency and improve energy conversion in the gasification process (Islam, 2020). Other studies also show that using catalysts in down-draft gasifiers can optimize gasification parameters, increase CGE, and produce higher-quality gas (Ramos and Rouboa, 2020)

Overall, the use of catalysts not only improves gasification efficiency but also positively affects the quality of the produced gas, making it an effective strategy for generating cleaner and more efficient energy from biomass.

Comparative analysis with other catalysts (nickel, cobalt, zinc)

This study compares the performance of Al/Fe-pillared bentonite with other metal-based catalysts, such as Ni, Co, and Zn, as reported in the literature. According to Faizan and Song (2023), the Ni catalyst demonstrated enhanced gasification efficiency through tar reforming and an improved H₂/CO ratio. Meanwhile, Co and Zn catalysts were found to produce high-quality syngas with a higher H₂ and CO content compared to non-catalytic conditions (Kwon et al., 2024). The advantage of Al/Fe-pillared bentonite lies in its high thermal stability, its ability to reduce tar, and its more economical nature compared to the Ni catalyst. Moreover, this catalyst is more

environmentally friendly because it is based on natural materials and has a high level of sustainability, given the abundance of its raw materials in nature. These factors make Al/Fe-pillared bentonite a more affordable option for large-scale applications. The data is shown in Table 5.

The Al/Fe-pillared bentonite catalyst provides an economical and environmentally friendly alternative for biomass gasification applications. This material maintains thermal stability and improves syngas quality without the high costs associated with transition metal catalysts.

Catalyst stability after reuse

The stability of the catalyst after several cycles of use has not been directly tested in this study. However, based on the literature, bentonite-based catalysts, including those modified with Al and Fe, are known to have structures capable of withstanding high thermal conditions and possess good regeneration potential after operational cycles. This is due to the intercalation of metals, which enhances the mechanical strength and structural stability of bentonite (Bellucci et al., 2023). Therefore, it is expected that Al/Fe-pillared bentonite will exhibit similar stability in long-term applications. To address this limitation, it is recommended to conduct long-term stability tests, including the evaluation of structural changes using XRD and FTIR after several cycles of use. Such a study would provide quantitative data on the catalyst’s performance during repeated use.

CONCLUSIONS

This study demonstrates that Al/Fe-pillared bentonite significantly enhances the efficiency of EFB gasification, addressing key challenges such as high tar formation and incomplete carbon conversion. By modifying bentonite with acid activation and metal pillaring, the material’s physicochemical properties – including thermal

Table 5. Comparative performance of Al/Fe-Pillared bentonite with other catalysts (Ni, Co, Zn) in biomass gasification

Parameter	Al/Fe-pillared bentonite	Ni catalyst	Co catalyst	Zn catalyst
H ₂ content (%)	36.1	42.3	38	35.6
Tar reduction (%)	40.2	55.3	48.7	37.2
Material cost	Low	High	Medium	Medium
Cycle durability	High	Medium	High	High

stability, porosity, and catalytic activity – were significantly improved. The use of Al/Fe-pillared bentonite as a catalyst in the gasification process led to a substantial increase in the production of valuable syngas components such as H₂ and CO while reducing tar formation. This catalyst also improves carbon conversion efficiency without the high costs typically associated with metal-based catalysts. These findings offer a cost-effective and environmentally friendly solution for enhancing biomass gasification, with potential applications for large-scale renewable energy production. Future research could focus on optimizing the metal pillar concentrations, evaluating the catalyst's performance over multiple cycles, and investigating its use with different biomass feedstocks to further increase syngas quality and process efficiency. Additionally, studying the catalyst's performance in real-world gasification systems and its recyclability could help develop more sustainable and efficient biomass-to-energy technologies.

Acknowledgments

This research was funded by the- Ministry of Education, Culture, Research, and Technology of the Republic of Indonesia through the Doctoral Dissertation Research scheme (Contract Number: 164/E5/PG.02.00.PL/2023 and 0143.01/UN9/SB3.LP2M.PT/2023).

REFERENCES

- Amari, A., Alzahrani, F. M., Katubi, K. M., Alsaiani, N. S., Tahooun, M. A., & Rebah, F. Ben. (2021). Clay-polymer nanocomposites: Preparations and utilization for pollutants removal. In *Materials* 14(6). MDPI AG. <https://doi.org/10.3390/ma14061365>
- Aprianti, N., Faizal, M., Said, M., & Nasir, S. (2024). Sorption-enhanced steam gasification of fine coal waste for fuel producing. *Journal of King Saud University - Engineering Sciences*, 36(2), 81–88. <https://doi.org/10.1016/j.jksues.2022.08.003>
- Asadullah, M., Miyazawa, T., Ito, S. I., Kunimori, K., Yamada, M., & Tomishige, K. (2004). Gasification of different biomasses in a dual-bed gasifier system combined with novel catalysts with high energy efficiency. *Applied Catalysis A: General*, 267(1–2), 95–102. <https://doi.org/10.1016/j.apcata.2004.02.028>
- Bellucci, S., Rudayni, H. A., Shemy, M. H., Aladwani, M., Alneghery, L. M., Allam, A. A., & Abukhadra, M. R. (2023). Synthesis and characterization of green zinc-metal-pillared bentonite mediated curcumin extract (Zn@CN/BE) as an enhanced antioxidant and anti-diabetes agent. *Inorganics*, 11(4). <https://doi.org/10.3390/inorganics11040154>
- Berhe, M. T., Berhe, G. G., Cheru, M. S., & Weldehans, M. G. (2024). Characterization of acid activation of bentonite clay of Hadar, Afar, Ethiopia. *Advances in Materials Science and Engineering*, 1. <https://doi.org/10.1155/2024/6413786>
- Borah, D., Nath, H., & Saikia, H. (2022). Modification of bentonite clay & its applications: a review. In *Reviews in Inorganic Chemistry* 42(3), 265–282. De Gruyter Open Ltd. <https://doi.org/10.1515/revic-2021-0030>
- Crespo, E., Martín, D. A., & Costafreda, J. L. (2024). Bentonite clays related to volcanosedimentary formations in southeastern Spain: Mineralogical, Chemical and Pozzolanic Characteristics. *Minerals*, 14(8). <https://doi.org/10.3390/min14080814>
- Cuevas, J., Cabrera, M. Á., Fernández, C., Mota-Heredia, C., Fernández, R., Torres, E., Turrero, M. J., & Ruiz, A. I. (2022). Bentonite Powder XRD Quantitative Analysis Using Rietveld Refinement: Revisiting and Updating Bulk Semiquantitative Mineralogical Compositions. *Minerals*, 12(6). <https://doi.org/10.3390/min12060772>
- Ebrahimi, P., Kumar, A., & Khraisheh, M. (2020). A review of recent advances in water-gas shift catalysis for hydrogen production. *Emergent Materials*, 3, 881–917. <https://doi.org/10.1007/s42247-020-00116-y/Published>
- Faizan, M., & Song, H. (2023). Critical review on catalytic biomass gasification: State-of-Art progress, technical challenges, and perspectives in future development. *Journal of Cleaner Production*, 408, 137224.
- Gandhi, D., Bandyopadhyay, R., & Soni, B. (2022). Naturally occurring bentonite clay: Structural augmentation, characterization and application as catalyst. *Materials Today: Proceedings*, 57, 194–201. <https://doi.org/10.1016/j.matpr.2022.02.346>
- Gao, N., Salisu, J., Quan, C., & Williams, P. (2021). Modified nickel-based catalysts for improved steam reforming of biomass tar: A critical review. In *Renewable and Sustainable Energy Reviews* 145. Elsevier Ltd. <https://doi.org/10.1016/j.rser.2021.111023>
- Ihekwe, G. O., Shondo, J. N., Orisekeh, K. I., Kalu-Uka, G. M., Nwuzor, I. C., & Onwualu, A. P. (2020). Characterization of certain Nigerian clay minerals for water purification and other industrial applications. *Heliyon*, 6(4). <https://doi.org/10.1016/j.heliyon.2020.e03783>
- Islam, M. W. (2020). A review of dolomite catalyst for biomass gasification tar removal. In *Fuel* 267. Elsevier Ltd. <https://doi.org/10.1016/j.fuel.2020.117095>

15. Keereerak, A., Sukkhata, N., Lehman, N., Nakaramontri, Y., Sengloyluan, K., Johns, J., & Kalkornsurapranee, E. (2022). Development and characterization of unmodified and modified natural rubber composites filled with modified clay. *Polymers*, *14*(17). <https://doi.org/10.3390/polym14173515>
16. Kurian, M., & Kavitha, S. (2016). A Review on the Importance of Pillared Interlayered Clays in Green Chemical Catalysis. *IOSR Journal of Applied Chemistry*, 47–54. www.iostjournals.org
17. Kwon, T., Jeong, H., Kim, M., Jung, S., & Ro, I. (2024). Catalytic approaches to tackle mixed plastic waste challenges: A review. *Langmuir*, *40*(33).
18. Liu, Q., Hu, C., Peng, B., Liu, C., Li, Z., Wu, K., Zhang, H., & Xiao, R. (2019). High H₂/CO ratio syngas production from chemical looping co-gasification of biomass and polyethylene with CaO/Fe₂O₃ oxygen carrier. *Energy Conversion and Management*, *199*, 111951. <https://doi.org/10.1016/j.enconman.2019.111951>
19. Liu, Z., Zhang, Y., Lee, J., & Xing, L. (2024). A review of application mechanism and research progress of Fe/montmorillonite-based catalysts in heterogeneous Fenton reactions. In *Journal of Environmental Chemical Engineering* *12*(2). Elsevier Ltd. <https://doi.org/10.1016/j.jece.2024.112152>
20. Lu, Q., Li, W., Zhang, X., Liu, Z., Cao, Q., Xie, X., & Yuan, S. (2020). Experimental study on catalytic pyrolysis of biomass over a Ni/Ca-promoted Fe catalyst. *Fuel*, *263*, 116690.
21. Maitlo, G., Ali, I., Mangi, K. H., Ali, S., Maitlo, H. A., Unar, I. N., & Pirzada, A. M. (2022). Thermochemical conversion of biomass for syngas production: Current status and future trends. In *Sustainability (Switzerland)* *14*(5). MDPI. <https://doi.org/10.3390/su14052596>
22. Mane, P. V., Rego, R. M., Yap, P. L., Losic, D., & Kurkuri, M. D. (2024). Unveiling cutting-edge advances in high surface area porous materials for the efficient removal of toxic metal ions from water. In *Progress in Materials Science* *146*. Elsevier Ltd. <https://doi.org/10.1016/j.pmatsci.2024.101314>
23. Nganda, A., Srivastava, P., Lamba, B. Y., Pandey, A., & Kumar, M. (2023). Advances in the fabrication, modification, and performance of biochar, red mud, calcium oxide, and bentonite catalysts in waste-to-fuel conversion. *Environmental Research*, *232*(116284).
24. Ramos, A., & Rouboa, A. (2020). Syngas production strategies from biomass gasification: Numerical studies for operational conditions and quality indexes. *Renewable Energy*, *155*, 1211–1221. <https://doi.org/10.1016/j.renene.2020.03.158>
25. Said, M., Dian, A. R., Mohadi, R., & Lesbani, A. (2020). Cr/Al Pillared Bentonite and Its Application on Congo Red and Direct Blue Removal. *Molekul*, *15*(3), 140–148.
26. Taghavi, R., Rostamnia, S., Farajzadeh, M., Karimi-Maleh, H., Wang, J., Kim, D., Jang, H. W., Luque, R., Varma, R. S., & Shokouhimehr, M. (2022). Magnetite metal-organic frameworks: Applications in environmental remediation of heavy metals, organic contaminants, and other pollutants. *Inorganic Chemistry*, *61*(40), 15747–15783. <https://doi.org/10.1021/acs.inorgchem.2c01939>
27. Vallejo, C. A., Galeano, L. A., Trujillano, R., Vicente, M. Á., & Gil, A. (2020). Preparation of Al/Fe-PILC clay catalysts from concentrated precursors: Enhanced hydrolysis of pillaring metals and intercalation. *RSC Advances*, *10*(66), 40450–40460. <https://doi.org/10.1039/d0ra08948f>
28. Wang, B., Lan, J., Bo, C., Gong, B., & Ou, J. (2023). Adsorption of heavy metal onto biomass-derived activated carbon: review. In *RSC Advances* *13*(7), 4275–4302. Royal Society of Chemistry. <https://doi.org/10.1039/d2ra07911a>
29. Wang, J., Kang, D., Shen, B., Sun, H., & Wu, C. (2020). Enhanced hydrogen production from catalytic biomass gasification with in-situ CO₂ capture. *Environmental Pollution*, *267*. <https://doi.org/10.1016/j.envpol.2020.115487>
30. Wei, G., Yang, Y., Li, Y., Zhang, L., Xin, Z., Li, Z., & Huang, L. (2020). A new catalytic composite of bentonite-based bismuth ferrites with good response to visible light for photo-Fenton reaction: Preparation, characterization and analysis of physicochemical changes. *Applied Clay Science*, *184*(105397).
31. Wu, N., Lan, K., & Yao, Y. (2023). An integrated techno-economic and environmental assessment for carbon 1 capture in hydrogen production by biomass gasification 2. *Resources, Conservation and Recycling*, *188*(106693).
32. Yuan, D., Peng, Y., Ma, L., Li, J., Zhao, J., Hao, J., Wang, S., Liang, B., Ye, J., & Yaguang, L. (2022). Coke and sintering resistant nickel atomically doped with ceria nanosheets for highly efficient solar driven hydrogen production from bioethanol. *Green Chemistry*, *5*, 1749–2252.